

# STRUCTURAL DESIGN OF OFFSHORE WIND FARM IN DC TRANSMISSION

Alireza Alizadeh Kiapi

Department of Electrical Engineering, K. N. Toosi University of Technology, KNTU, Tehran, Iran

**Abstract:** In this study, a new method for power transfer in offshore wind farms is proposed. The proposal includes a parallel arrangement of conventional synchronous generators with excitation coils and a DC/DC converter, which eventually is connected to a HVDC transmission system. The excitation coil is fed by a DC link through a power electronic DC/DC converter. Then the system is modeled using the state space of the system. Dynamic and transient response of proposed structure is evaluated based on simulation results. Simulation results show that the proposed model matches the real system properly.

**Keywords:** Synchronous generator, back-to-back converter, DC link, HVDC

## I. INTRODUCTION

In recent years, the micro grids are employed in power system to supply the power demand with lower cost and losses. Offshore wind farm micro grids have recently attracted attentions as a renewable source of energy. Based on the technical and economical studies, AC or DC transfer of energy from large offshore wind farms to the power network is carried out to avoid additional AC / DC conversion that is associated with energy losses and cost.

The distance between these wind farms and their long distances from the power transmission system make it difficult to use long-air transmissions, and therefore the only remaining way to transport electric energy produced by wind farms is the sea cables that has high capacity capacitance [1]. If these lines are used as AC, then there should be compensators for the reactive power at both ends and also in the middle of the line. In contrary, in DC transmission, the capacitors would not only make no problems in terms of reactive current, but also help the stability of system against transmission system transients [2]. The use of HVDC technology as an offshore wind farm transmission line requires AC / DC conversion terminals, which leads to high cost HVDC technology in near distance. Recent studies shown that for distances greater than 60-50 km, the cost of compensators and the AC transmission line with a three-phase cable goes up to an extent that replacing the AC transmission line with the DC transmission line also finds economic justification and comes with many benefits[3-5].

It should be noted that with the advance of power electronics devices and the cost of AC / DC conversion terminals is reduced, and it might be expected that HVDC technology will be used in the near future for shorter lines. It can be predicted with certainty that in the near future, most of the large offshore wind farms will be connected to the transmission system the HVDC technology [6]. Also, as demand side control strategy getting mature day by day,

penetration of these sources of energy speeds up[7][8]. However, due to uncertain characteristics of renewables, careful planning needs to be implemented to make the power system robust against uncertainty[9-11]

Technically, the internal network of wind farms can also be used for DC or AC technology. On the other hand, the absence of local consumers makes the choice of the internal network type for the offshore farms to be determined by the designer. Therefore, it can be seen that in existing fields, both AC and DC networks have been used [12].

In the case of using a DC transmission with an AC network, an AC to DC converter will be inevitable at the point where the wind farm is connected to the transmission line. Considering the losses caused by the AC / DC conversion and the discussion of the reduction of the excessive conversions in the power grid, it can be concluded that the choice of the local DC network for offshore wind farms with the HVDC transmission line is not only efficient in term of energy, but also it eliminates the need for an AC to DC conversion terminal at the local network connection to the transmission line and reduces the investment cost. Of course, this conclusion is correct if the output of each wind turbine is not AC [13]. The choice of a local DC network makes it possible to remove a DC/AC conversion phase which is necessary at the electrical terminal of wind turbines and at the point where they are connected to the AC network. As a result, most of the energy losses and investment costs will be reduced [14].

Moreover, there are some optimization algorithms that show the best location for placing renewable resources in the system to make the total costs that should be paid by government to its minimum amount [15].

In this study, a new method for power transfer in offshore wind farms is proposed. Dynamic and transient response of proposed structure is evaluated based on simulation results. This paper is organized as follows; in the section the proposed structure will be introduced. The model of proposed structure will be presented in section III. Simulation results are demonstrated in section IV. Finally, the conclusion is given in section V.

## II. PROPOSED STRUCTURE OF OFFSHORE WIND FARM

The Electric generator in the proposed structure is a wound rotor type that can be with or without a gearbox. AC electric power at the three-phase stator terminal of this generator is rectified through a three-phase diode bridge and delivered to a local DC network. The control of this generator is done through a DC / DC converter, which is located between the rotor actuator and the local DC network (Fig. 1)

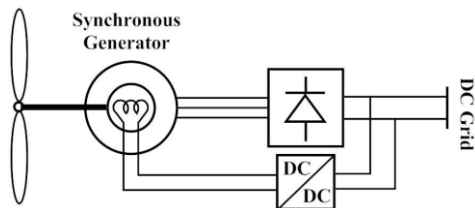


Fig.1 Electrical part of proposed wind turbine structure  
 The new structure DC / DC converter will have a nominal power as much as the nominal power of the coil excites the generator or just beyond that. Therefore, the generator controller converter is chosen with a nominal capacity of 5 to 6 percent of the rated power of the wind turbine, and a DC / DC converter is simpler than the three-phase converter. On the other hand, the rectifying task which was used to be done by back to back converter in the common turbines, is now assigned to the diode bridge connected to the generator terminal, that is much less expensive than the converter of the common turbines (back-to-back VSC converter) (Fig. 2). It must be noted for medium voltage applications, isolated modular multilevel converter based DC / DC converters are proven to be preferred solutions [16].

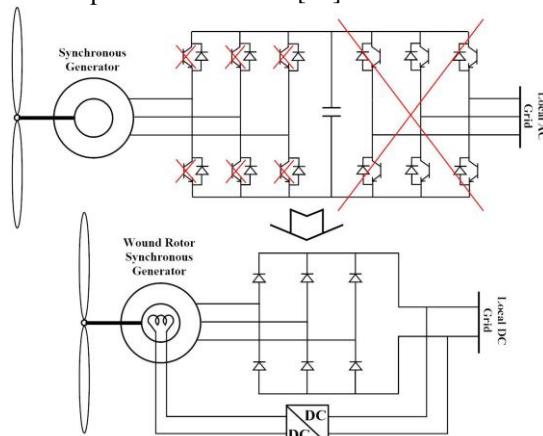


Fig.2 Comparison of proposed model and the conventional one

In this way, it is seen that in the new structure, the cost of the wind turbine converter will be significantly lower than that of the wind turbine with the conventional synchronous generator, and the cost of the electrical portion of generator will remain unchanged compared to the turbines. Therefore, the total cost of the turbine will decrease

In conjunction with the control structure used in the new wind turbine, it is necessary to point out that according to the concept of control of synchronous generator excitation, it may be thought that this option is more suitable for controlling reactive power and would not affect the actual power as much. In other words, at first it seems that by controlling the current of the wind turbine synchronous generator, it is not possible to control the actual power and eventually MPPT [17][18].

However, considering the diode bridge of the generator terminal, it is observed that the generator operation will always be carried out with a power factor of one and a reactive power of zero, and the effect of the change of excitation current will not affect the reactive power of the generator. Thus, keeping the current and voltage phase the

same through the diode bridge of the generator terminal, changes in the excitation current, which is the same as the change in the internal voltage of the generator stator, leads to a change in the current magnitude and eventually the actual change of the generator terminal power. The potential benefits expected from the new structure are [19]:

Significant reduction in wind turbine prices

Possibility of faster response to transients and wind speed variations due to the strong and fast control of the excitation current that is supplied through the DC voltage of the local area network and the DC / DC converter on the actuator that can make the excitation current (wind turbine control parameter) to change quickly.

Possible disadvantages of this structure include:

The slip ring of generator excitation coil can cause a low reliability and high maintenance for a turbine generator compared with the PMSG generator.

There may be restrictions on the generation of harmonics injected into generators due to the use of a diode bridge for the generator.

In relation to the first disadvantage and the problem of sliprings, first of all, in wind turbines with a high number of poles without a gearbox, because of the relatively low speed of the rotor of the generator, compared to the wind turbines of the induction generator with gearbox (which means the lower number of rotor turns during a year), the problem of erosion of the slip ring is not as large as the induction generators. Secondly, the problem can be solved with the use of slip ring free excitation technology, which is a solution to synchronous generators, and solves the problem at low cost.

As it is seen in Fig. 3, in the new wind farm, rectifier converters GTO switches on the wind turbine output are replaced with a full diode bridge rectifier, which is expected to result in a significant reduction in costs in this section. The full diode-bridge rectifier connects the new structure via an inductor and operates as a current source. On the other hand, the excitation of the rotor in the new structure is carried out through a DC / DC converter with a nominal power of some percentages of the nominal power of the turbine, which is fed from the local network and is responsible for controlling the generator excitation to apply MPPT and other necessary turbine controls. It is obvious that the cost of this converter will be negligible with regard to its low nominal power compared to the reduction in the cost of the turbine converter. Also, Fig. 3 shows that VSC is used to connect the wind farm through HVDC line to the AC grid. The dynamic modeling of the VSC and its transient performance due to uncertainty of the wind power is discussed in [20].

In continue, modeling and simulation of the proposed structure will be discussed and the simulation results will be presented.

### III. MODELLING OF PROPOSED STRUCTURE

First connection of a voltage source with a diode bridge through an inductor is investigated. At this stage, it is assumed that there is a large capacitor at the rectifier side. This capacitor acts like a voltage source and its voltage is almost constant. This is in contrast to the usual mode, which usually exists at the rectifier side of the inductor, and the

current is usually constant. After the capacitor, an inductor can be used to reduce the ripple of DC current. As will be seen, the presence of a capacitor will reduce the current ripple as well as providing a DC voltage to the buck converter.

After considering the equations with the same inductance in the d and q axes, these equations will be extended in general for different reactances, and a model will be extracted in this case, then this model will be linearized, and its accuracy is checked.

In continue the dynamic of buck converter is investigated and it will be observed that the buck converter is much faster than the oscillation of the generator itself, and therefore the excitation voltage can be considered as a constant signal, which has no dynamic. Then a suitable controller for the excitation voltage will be designed to allow the power to be set at the desired value. The controller will then be used to simulate the overall system and the system response will be checked for different wind speed variations.

**A. Evaluating the Size of Capacitor**

In Fig. 4, a three-phase rectifier of a full-wave diode is shown in connection with a three-phase voltage source and source inductor. The presence of a capacitor C reduces the output voltage ripple and therefore the  $v_{dc}$  voltage is almost flat. On the other hand, the presence of inductor L reduces the current ripple and therefore the output current is approximately DC. DC load is initially modeled as a constant voltage source, as shown in Fig. 4. The value of this DC voltage is equal to

$$V_{dc} = V_d + RI_{dc} \tag{1}$$

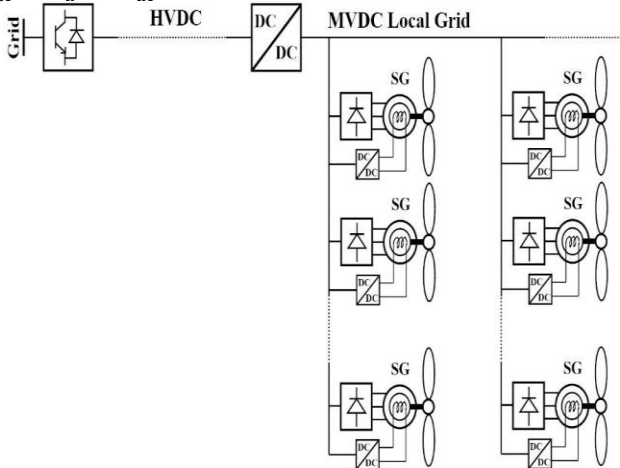


Fig.3 Structural of proposed offshore wind farm in DC transmission

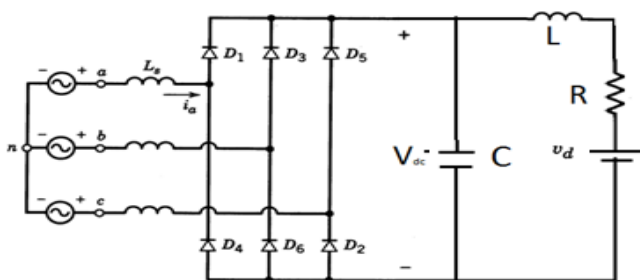


Fig.4 Full bridge rectifier

There are various ways to rectify the generator output voltage, and each of which may have different costs, advantages and disadvantages. The easiest way is to use a diode bridge. In front of a diode bridge you can use an inductor or capacitor. If the inductor is used, the DC side will act like a current source and the AC side current ripple will also be high and will require the use of large AC filters. But if the capacitor is used, the DC side will act like a voltage source, and the current harmonic level will decrease on the AC side. In this situation, you will not need an AC filter, or the filter used will be very small. Now, it may be a question of how much capacitance will be used and how much is practical

The frequency of the rectified voltage is six times the AC frequency. In a time equal to half of a period, the capacitor voltage reduction will be equal to:

$$\Delta V = \frac{1}{C} \int_0^{\frac{1}{12f}} I_{dc} dt \Rightarrow \frac{\Delta V}{V} = \frac{P}{12fCV^2} \tag{2}$$

Of course, since the frequency of the wind turbine generators is less than 50 Hz, the amount of capacitance required is large. Another option is the use of high frequency keys, which will be associated with increased costs. However, at a frequency of about 1 KHz for switches, the capacitance value is reduced, but instead the AC filters are needed.

**B. Power Transfer Capability**

The amount of power in per unit can be obtained from the following relationships:

$$P = E_L I_1 \cos(\theta_{I1}) \tag{3}$$

$$Q = E_L I_1 \sin(\theta_{I1}) - X I_1^2 \tag{4}$$

In which  $E_L$  is the effective value of the source voltage,  $I_1$  and  $\theta_{I1}$  are the fundamental current harmonic magnitude and angle.

In Fig.5, the magnitude and angle of the current are plotted, and in Fig. 6, the active and reactive power of the terminal is plotted for  $X = 1$ .

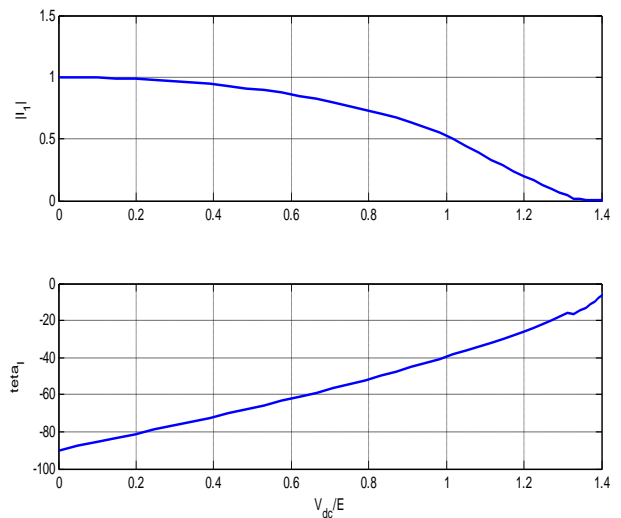


Fig.5 Magnitude and phasor of fundamental harmonic

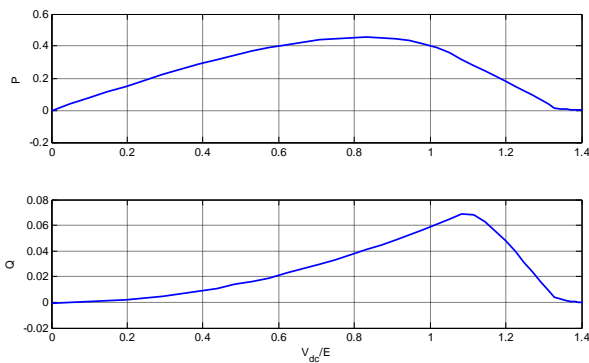


Fig.6 Generated active and reactive power

As can be seen, the magnitude of the current decreases with increasing  $\frac{V_{dc}}{E}$  ratio, but along with that, the power factor also decreases. As a result, the transferred power capacity is initially increased and then reduced. It is also observed that the reactive power produced at the terminal is very small and the load power factor is approximately equal to one. The active power produced at the point  $\frac{V_{dc}}{E} = 0.83$  has a maximum value of 0.45 pu. If the value of X changes, the point is the same, but the maximum value will be  $0.45/X$ . At this point, the THD has a low amount of 4.2%, and the circuit performance at this point is seems to be the best. Therefore, to use the full system capacity, the systems should be designed so that it works at the highest possible capacity in peak power demand. On the other hand, at this point, the power gradient is approximately zero in relation to the value of  $V_{dc}$ , which means that its changes has very small effect on for power, which is also a desirable case. Although the given point is a maximum, it is observed the same characteristics with a small difference in the range of  $0.6 < \frac{V_{dc}}{E} < 1$ . In the following, we will examine the dynamic situation.

Assuming E is aligned with the q axis so,

$$E_q = \frac{\sqrt{2}}{\sqrt{3}} E_L \tag{5}$$

$$E_d = 0 \tag{6}$$

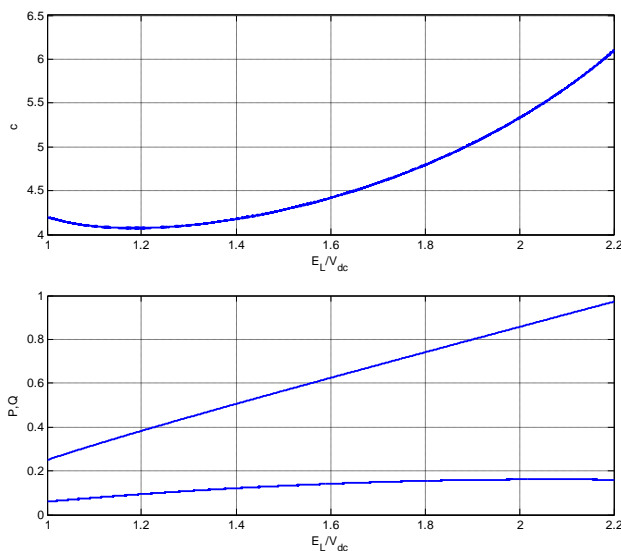


Fig.7 Variation of parameter c and active and reactive power

And the terminal voltage in dq reference frame is calculated as:

$$V_q = \frac{\sqrt{2}}{\sqrt{3}} V_{L1} \cos(\delta) \tag{7}$$

$$V_d = -\frac{\sqrt{2}}{\sqrt{3}} V_{L1} \sin(\delta) \tag{8}$$

The line voltage is selected as the base voltage on the AC side. The base voltage on the DC side is chosen so that the DC voltage DC of 1 pu produces the AC voltage AC of 1 pu. So;

$$V_{dc,b} = \frac{V_b}{0.78} \tag{9}$$

If the ratio of active and reactive power used in all loads is equal to c.

$$\frac{P}{Q} = c \tag{10}$$

c is relatively constant in low loads and has a gradient equal to active power in large loads. A graph of a sample c is shown in Fig. 7 by simulating slow changes of  $E_L/V_{dc}$  along with active and reactive power changes. By obtaining graph c and assuming that there is no significant difference between the dynamic and static states, static and dynamic equations can be attained as:

$$\frac{V_d I_d + V_q I_q}{V_q I_d - V_d I_q} = c \tag{11}$$

Another relationship that needs to be considered to find relationships is the magnitude of the voltage at the converter side, which is relatively constant; so,

$$V_d^2 + V_q^2 = V_{dc}^2 \tag{12}$$

So using (9-10) will result in:

$$V_d = \frac{V_{dc}}{\sqrt{1 + c^2 I}} (c I_d - I_q) \tag{13}$$

$$V_q = \frac{V_{dc}}{\sqrt{1 + c^2 I}} (I_d + c I_q) \tag{14}$$

Other relations can be obtained from the generator's internal equations. It should be noted that in this case, the generator does not need a damper. Since these windings are needed for synchronization, and help the generator to rotate at the nominal frequency of the network. But here there is no need for synchronization, because there is not at all a network with a certain frequency that the generator wants to synchronize with it. Therefore, the equations of the synchronous generator are written in conjunction with the excitation coil, and regardless of the damping windings [21]:

$$V_d = \frac{1}{\omega_b} \frac{d}{dt} \psi_d - \psi_q \omega_r - R I_d \tag{15}$$

$$V_q = \frac{1}{\omega_b} \frac{d}{dt} \psi_q + \psi_d \omega_r - R I_q \tag{16}$$

$$E_{fd} = \frac{1}{\omega_b} \frac{d}{dt} \psi_{fd} + R_{fd} I_{fd} \tag{17}$$

where

$$\psi_d = -L_d I_d + L_{ad} I_{fd} \tag{18}$$

$$\psi_q = -L_q I_q \tag{19}$$

$$\psi_{fd} = L_{fd} I_{fd} - L_{ad} I_d \tag{20}$$

Substituting the flux expressions in (15-17) will result in:

$$V_d = -L_d \frac{1}{\omega_b} \frac{d}{dt} I_d + L_q \omega_r I_q - R I_d + L_{ad} \frac{1}{\omega_b} \frac{d}{dt} I_{fd} \quad (21)$$

$$V_q = -L_q \frac{1}{\omega_b} \frac{d}{dt} I_q - L_d \omega_r I_d - R I_q + L_{ad} \frac{1}{\omega_b} \frac{d}{dt} I_{fd} \quad (22)$$

$$E_{fd} = L_{fd} \frac{1}{\omega_b} \frac{d}{dt} I_{fd} + R_{fd} I_{fd} - L_{ad} \frac{1}{\omega_b} \frac{d}{dt} I_d \quad (23)$$

After some simplification the following are attained.

$$I_d = \frac{-V_d + L_q \omega_r I_q + \frac{L_{ad}}{L_{fd}} (E_{fd} - R_{fd} I_{fd})}{s \frac{L_d}{\omega_b} + R} \quad (24)$$

$$I_q = \frac{-V_q - L_d \omega_r I_d + L_{ad} \omega_r I_{fd}}{s \frac{L_q}{\omega_b} + R} \quad (25)$$

$$I_{fd} = \frac{1}{R_{fd}} \frac{E_{fd} - \frac{L_{ad}}{L_d} (V_d + R I_d - L_q \omega_r I_q)}{s \frac{T_d}{\omega_b} + 1} \quad (26)$$

where

$$L_d = L_d - \frac{L_{ad}^2}{L_{fd}} \quad (27)$$

$$T_d = \frac{L_{fd} - \frac{L_{ad}^2}{L_d}}{R_{fd}} \quad (28)$$

The mechanical equations are:

$$2H \frac{d\omega_r}{dt} = T_m - T_e - K_D \omega_r \quad (29)$$

where

$$T_e = (\psi_d I_q - \psi_q I_d) = L_{ad} I_{fd} I_q + (L_q - L_d) I_d I_q \quad (30)$$

### C. Dynamic Model

Although the calculated C in the previous section was in static mode, this model is also valid for dynamic mode. Because, as mentioned, the model has no dynamics, and so has the same static and dynamic model. On the other hand, C has a lot of changes, but there is some point that increases the accuracy of the model in using C as constant value. If C is small, its variation is small and therefore C is small and constant in low power. But if C is large, it can be written as:

$$V_d = \frac{V_{dc}}{\sqrt{1 + C^2 I}} (c I_d - I_q) \cong \frac{V_{dc}}{I} I_d \quad (31)$$

$$V_q = \frac{V_{dc}}{\sqrt{1 + C^2 I}} (I_d + c I_q) \cong \frac{V_{dc}}{I} I_q \quad (32)$$

which shows that relations are independent of considering a large value for c. Therefore, in general, c can be considered as a constant in dynamic equations. If we assume the voltage source and the diode like a load, it lacks any dynamic and its dynamic and static conditions are the same. Since neither the diode nor the voltage source are dynamic elements. The only change that can be made to them is the small change of DC voltage due to the fluctuations in the DC side, which will be added to the model.

In continue the existing relationships are linearized. Linearization of the relationships helps to better understand the system transient response and its characteristics, and to examine the stability and design of the controller. To linearize each parameter is considered as the sum of a constant DC values and a small amount of turbulence. For example, for DC voltage

$$v_{dc} = V_{dc} + \widehat{v}_{dc} \quad (33)$$

In the following, the DC component relations are canceling each other, and regardless of the second-order terms, the equations can be completely linearized. By linearizing the relationship of the voltage, one can write:

$$\widehat{v}_d = \frac{V_{dc}}{\sqrt{1 + C^2 I^3}} \left( (c I_q^2 + I_d I_q) \widehat{t}_d - \right) + \frac{V_d}{V_{dc}} \widehat{v}_{dc} \\ = K_1 \widehat{t}_d - K_2 \widehat{t}_q + \frac{V_d}{V_{dc}} \widehat{v}_{dc} \quad (34)$$

$$\widehat{v}_q = \frac{V_{dc}}{\sqrt{1 + C^2 I^3}} \left( (I_q^2 - c I_d I_q) \widehat{t}_d + \right) + \frac{V_q}{V_{dc}} \widehat{v}_{dc} \\ = K_3 \widehat{t}_d - K_4 \widehat{t}_q + \frac{V_q}{V_{dc}} \widehat{v}_{dc} \quad (35)$$

The generator equations around the operating point are simplified as

$$\widehat{t}_d = \frac{-\widehat{v}_d + L_q \omega_r \widehat{t}_q + L_q \widehat{\omega}_r I_q + \frac{L_{ad}}{L_{fd}} (\widehat{e}_{fd} - R_{fd} \widehat{t}_{fd})}{s \frac{L_d}{\omega_b} + R} \quad (36)$$

$$\widehat{t}_q = \frac{-\widehat{v}_q - L_d \omega_r \widehat{t}_d + L_{ad} \omega_r \widehat{t}_{fd} + (L_{ad} I_{fd} - L_d I_d) \widehat{\omega}_r}{s \frac{L_q}{\omega_b} + R} \quad (37)$$

$$\widehat{t}_{fd} = \frac{1}{R_{fd}} \frac{\widehat{e}_{fd} - \frac{L_{ad}}{L_d} (\widehat{v}_d + R \widehat{t}_d - L_q \omega_r \widehat{t}_q - L_q \widehat{\omega}_r I_q)}{s \frac{T_d}{\omega_b} + 1} \quad (38)$$

Substituting (29), (30) in (35-37) will result in:

$$\widehat{t}_d = \frac{(K_2 + L_q \omega_r) \widehat{t}_q + L_q \widehat{\omega}_r I_q + \frac{L_{ad}}{L_{fd}} (\widehat{e}_{fd} - R_{fd} \widehat{t}_{fd}) - \frac{V_d}{V_{dc}} \widehat{v}_{dc}}{s \frac{L_d}{\omega_b} + R + K_1} \quad (39)$$

$$\widehat{t}_q = \frac{-(K_3 + L_d \omega_r) \widehat{t}_d + L_{ad} \omega_r \widehat{t}_{fd} + (L_{ad} I_{fd} - L_d I_d) \widehat{\omega}_r - \frac{V_q}{V_{dc}} \widehat{v}_{dc}}{s \frac{L_q}{\omega_b} + R + K_4} \quad (40)$$

$$\widehat{t}_{fd} = \frac{1}{R_{fd}} \frac{\widehat{e}_{fd} - \frac{L_{ad}}{L_d} \left( (K_1 + R) \widehat{t}_d - (K_2 + L_q \omega_r) \widehat{t}_q - L_q \widehat{\omega}_r I_q + \frac{V_d}{V_{dc}} \widehat{v}_{dc} \right)}{s \frac{T_d}{\omega_b} + 1} \quad (41)$$

Linearizing the mechanical equations will result in:

$$\widehat{\omega}_r = \frac{\widehat{T}_m - \widehat{T}_e}{2Hs + K_D} \quad (42)$$

And the electrical torque will be:

$$\widehat{T}_e = (L_q - L_d) I_q \widehat{t}_d + (L_{ad} I_{fd} + (L_q - L_d) I_d) \widehat{t}_q + L_{ad} I_q \widehat{t}_{fd} \quad (43)$$

The output power is calculated as:

$$P = V_d I_d + V_q I_q \quad (44)$$

The power equation is linearized around the operating point as

$$\hat{P} = V_d \hat{i}_d + I_d \hat{v}_d + V_q \hat{i}_q + I_q \hat{v}_q \quad (45)$$

And some simplification will result in:

$$\hat{P} = (V_d + K_1 I_d + K_3 I_q) \hat{i}_d + (V_q - K_2 I_d + K_4 I_q) \hat{i}_q + \frac{P}{V_{dc}} \hat{v}_{dc} \quad (46)$$

#### IV. SIMULATION RESULTS

To test the accuracy of the model, simulation is performed in three cases. First, the simulation of detailed model is being done. The second simulation assuming that the static and dynamic states of the diode are the same. The third simulation is the linearized model. For this purpose, graph C is attained by changing the excitation voltage. Then the nominal value of C is obtained in a given operating condition. In the next step, by writing nonlinear and linear equations in MATLAB, the simulation results of the detailed model and the linearized one are compared.

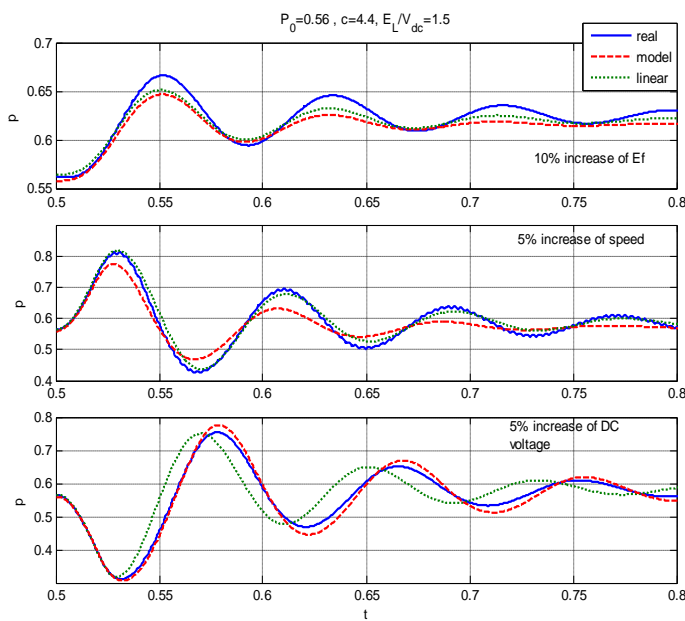


Fig. 8 Model accuracy at P=0.56 pu

The parameters of simulated generator are as follows:

$$S_b = 6.86MVA, V_b = 11KV, I_b = 360A, f_b = 50Hz$$

$$R = 1e-4, X_d = 1.6, X_q = 0.8, X_l = 0.14$$

$$X_{fd} = 1.574, R_{fd} = 0.03$$

Under the two loading conditions, P = 0.56 pu (first case) and P = 0.76 pu (second case), the system response to the step changes of 0.1pu in the magnitude of the exciting voltage, 0.05 pu at a speed and 0.05 pu at the DC voltage is simulated, and illustrated in Fig. 8 and 9. As can be seen, linearization has brought the linear model closer to the detailed model. Although the magnitude of the fluctuations may be different, but the frequencies and damping ratio are almost the same.

The poles in the first case are equal to:

$$-973, -10.57 \pm J77.16$$

The poles in the second case are equal to:

$$-752, -4.62 \pm J83.8$$

It is observed that there is always a fast pole, which is generally insignificant. In addition, there is a pair of conjugate poles, which increase corresponding frequency and decrease the damping ratio while increasing the power. It can be seen that by increasing the power and excitation voltage to a value of 2.2, the conjugate poles will be as follows:

$$-2.2 \pm J85$$

It is noticeable that the system is always stable, although its damping is very small at high power. It should be noted that mechanical specification was not modeled in this case. This will make the system unstable; since there is no speed controller. As can be seen, the variation of the oscillation frequency with the change in power is very low, while the damping in the high powers greatly decreases. Therefore, the most critical mode is in high power, where the attenuation is very small and the frequency of oscillations is high.

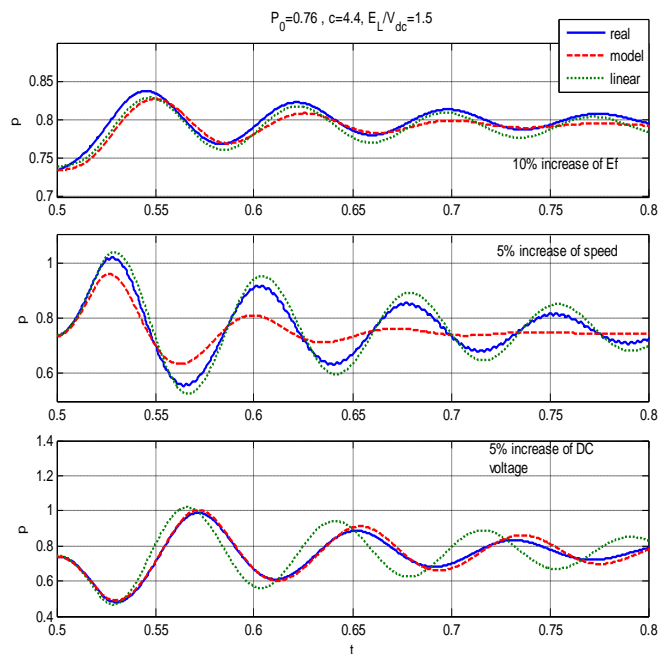


Fig. 9 Model accuracy at P=0.76 pu

#### V. CONCLUSIONS

In this paper, the proposed model for wind turbine electrical part and the method of matching the transmission of wind turbines and lines are introduced. Then the system is modeled using the state space of the system. The linearized model is simulated to evaluate its accuracy. Simulation results shows that the proposed model matches the detailed model for a good degree of accuracy.

#### REFERENCES

- [1] Bresesti, P., et al. "HVDC Connection of Offshore Wind Farms to the Transmission System." IEEE Transactions on Energy Conversion, Vol 22, Issue

- 1: 37-43, 2007.
- [2] Fujin Deng and Zhe Chen "An offshore wind farm with DC grid connection and its performance under power system transients" Power and Energy Society General Meeting, IEEE, 2011.
- [3] Das, D., J. Pan, and S. Bala. "HVDC Light for large offshore wind farm integration." In Power Electronics and Machines in Wind Applications (PEMWA), 2012 IEEE, pp. 1-7. IEEE, 2012.
- [4] S. Jafarishiadeh, M. Farasat, S. Mehraeen "Grid-connected operation of direct-drive wave energy converter by using HVDC line and undersea storage system" in Proc. Energy Conversion Congress and Exposition (ECCE), Cincinnati, OH, USA, pp. 5565-5571, 2017.
- [5] Bresesti, P., et al. "Transmission expansion issues for offshore wind farms integration in Europe" Transmission and Distribution Conference and Exposition, IEEE, 2008.
- [6] Chih-Ju, C., et al. "Comparative evaluation of the HVDC and HVAC links integrated in a large offshore wind farm - an actual case study in Taiwan" Industry Applications Society Annual Meeting (IAS), IEEE, 2011.
- [7] Amini, Mahraz, and Mads Almassalkhi. "Investigating delays in frequency dependent load control." Innovative Smart Grid Technologies-Asia (ISGT-Asia), 2016 IEEE. IEEE, 2016.
- [8] M.S. Modarresi, L. Xie, and C. Singh. "Reserves from Controllable Swimming Pool Pumps: Reliability Assessment and Operational Planning." Proceedings of the 51st Hawaii International Conference on System Sciences. 2018.
- [9] M. Ghanaatian; S. Lotfifard, "Control of Flywheel Energy Storage Systems in Presence of Uncertainties" IEEE Transactions on Sustainable Energy, 2018
- [10] Amini, Mahraz, and Mads Almassalkhi. "Trading off robustness and performance in receding horizon control with uncertain energy resources." Power Systems Computation Conference (PSCC). 2018.
- [11] M. S. Modarresi, T. Huang, H. Ming and L. Xie, "Robust phase detection in distribution systems," 2017 IEEE Texas Power and Energy Conference (TPEC), College Station, TX, 2017, pp. 1-5.
- [12] Carlson, O. and S. Lundberg "Integration of wind power by DC-power systems" Power Tech, IEEE Russia, 2005.
- [13] Shamsnia, A., Parniani, M. "A New Cost-Effective Wind Farm Structure with HVDC Link Preserving Technical Advantages of Advanced offshore Wind Farms" Renewable Energy and Power Quality Journal, No. 11, (RE&PQJ-11), March 2013
- [14] Patterson, B. T. "DC, Come Home: DC Microgrids and the Birth of the "Enernet" " Power and Energy Magazine, IEEE, Vol 10, Issue 6: 60-69, 2012.
- [15] N. Ghanbari; H. Mokhtari; S. Bhattacharya, "Optimizing Operation Indices Considering Different Types of Distributed Generation in Microgrid Applications", Energies 2018, 11, 894.
- [16] S. Jafarishiadeh, V. Dargahi, AK. Sadigh, M. Farasat, "Novel multi-terminal MMC-based dc/dc converter for MVDC grid interconnection," IET Power Electronics, vol. 11, no. 7, pp. 1266-1276, June 2018
- [17] M. a. Abdullah, a. H. M. Yatim, C. W. Tan, and R. Saidur, "A review of maximum power point tracking algorithms for wind energy systems," Renew. Sustain. Energy Rev., vol. 16, no. 5, pp. 3220-3227, Jun. 2012.
- [18] M. A. Abdullah and A. H. M. Yatim, "A study of maximum power point tracking algorithms for wind energy system," in 2011 IEEE Conference on Clean Energy and Technology (CET), 2011, pp. 321-326.
- [19] Wu, Guohong, Y. Tohbai, and T. Takahashi. "Construction and operational properties of offshore wind farm power generation system with self-commuted HVDC transmission.", International Conference on Power System Technology, pp. 1-6. IEEE, 2010.
- [20] P. M. Shabestari, S. Ziaeinejad and A. Mehrizi-Sani, "Reachability analysis for a grid-connected voltage-sourced converter (VSC)," 2018 IEEE Applied Power Electronics Conference and Exposition (APEC), San Antonio, TX, 2018, pp. 2349-2354.
- [21] M. Ghanaatian, A. Radan, "Modeling and simulation of Dual Mechanical Port machine" International Power Electronics, Drive Systems and Technologies Conference, 2013.